ISSN 1027-4510, Journal of Surface Investigation: X-ray, Synchrotron and Neutron Techniques, 2017, Vol. 11, No. 5, pp. 1050–1055. © Pleiades Publishing, Ltd., 2017.
Original Russian Text © Yu.F. Ivanov, V.E. Gromov, V.E. Kormyshev, S.V. Konovalov, E.V. Kapralov, 2017, published in Poverkhnost', 2017, No. 10, pp. 56–63.

Structure and Properties of a Low-Carbon Steel Surface Modified by Electric Arc Surfacing

Yu. F. Ivanov[a, b], V. E. Gromov[c, *], V. E. Kormyshev[c], S. V. Konovalov[c], and E. V. Kapralov[c]

[a] *Institute of High Current Electronics, Siberian Branch, Russian Academy of Sciences, Tomsk, 634055 Russia*
[b] *Tomsk National Research State University, Tomsk, 634050 Russia*
[c] *Siberian State Industrial University, Novokuznetsk, 654007 Russia*
**e-mail: gromov@physics.sibsiu.ru*

Received February 17, 2017

Abstract—The structural-phase state and the distribution of microhardness over the cross section of single and double coatings deposited onto martensitic Hardox 450 low-carbon steel by alloyed flux-cored wire, are studied using modern physical materials science. It is demonstrated that the microhardness of a double deposited layer 10 mm in thickness exceeds the microhardness of the base metal by more than three times. It is found that the improved mechanical properties of the deposited layer are due to the formation of a submicro- and nanodisperse martensitic structure containing iron borides forming a plate-type eutectic. Plates of iron boride Fe_2B are formed in the eutectic in a single deposited layer, and in a double-deposited layer, plates of FeB are formed. The existence of bend extinction contours, indicating the formation of internal stress fields at the interface between the phases of iron borides and α-iron borides, is revealed.

Keywords: nanostructure, phase composition, microhardness, electric arc surfacing, eutectic
DOI: 10.1134/S1027451017050287

INTRODUCTION

In most cases, parts of machines and mechanisms operate under conditions of wear, cavitation, cyclic loads, and corrosion at cryogenic or high temperatures, at which maximum stresses occur in the surface layers of the metal where the main stress concentrators are located. A promising technology aimed at extending the service life of structures by restoring worn parts is arc welding by a flux-cored wire, which is widely used in the repair of machine parts for various purposes: agricultural machinery, urban and railway transport, technological equipment, etc. [1]. For an informed choice of the material of coatings, which correspond to the conditions of their use, it is necessary to conduct detailed studies of their properties and structure [2–5].

The goal of this work is to analyze the phase composition, defect substructure, and mechanical properties of a layer welded on Hardox 450 steel by a boron-containing flux-cored wire.

EXPERIMENTAL

Steel Hardox 450, the elemental composition of which is presented in Table 1, is used as the base material; it is characterized by a low concentration of alloying elements, hence, it is easy to weld and process. Because of a special quenching system, the essence of which is the rapid cooling of a rolled sheet without subsequent tempering, a fine-grained structure of the steel and its high hardness are achieved. The steel thus effectively resists most types of wear. Surfacing was carried out with PP–1 flux-cored wire, the elemental composition of which is presented in Table 2. This procedure was performed in a protective gas atmosphere consisting of 98% of argon and 2% of carbon dioxide at a welding current of 250–300 A and an arc voltage of 30–35 V. The deposited layer was formed in one pass and in two passes.

The phase composition and the defect substructure of the steel and welded metal were studied by diffraction transmission electron microscopy (thin foil method) [6–9]. The foils were made from plates of the weld metal cut by the electric spark method (a layer located at half the thickness of the weld metal). Plates cut in this way were thinned to a thickness of ~200 nm (thin foil, which is necessary for analysis by transmission electron microscopy) by spraying the metal with an ion beam (argon) using an Ion Slicer setup (JEOL). The mechanical properties of the weld metal and steel were characterized by the microhardness value (the Vickers method, the load on the indenter of 5 N).

Table 1. Element composition of Hardox 450 steel (wt %); the remaining part is iron

C	Si	Mn	Cr	Ni	Mo	B	P	S
0.19–0.26	0.70	1.60	0.25	0.25	0.25	0.004	0.025	0.010

Table 2. Element composition of PP-1 welding wire (wt %)

C	Mn	Si	Ni	B	Fe
0.7	2.0	1.0	2.0	4.5	Remaining

RESULTS AND DISCUSSION

Structure of the workpiece volume. Steel Hardox 450 is designed for operation under conditions that impose special requirements for wear resistance in combination with good cold bending and weldability. The steel's high hardness is achieved by means of a special sheet quenching system, after which the metal acquires a martensitic structure.

The formation of a layer deposited onto the surface of steel by the electric arc method is accompanied by poorly controlled heating of the material. This leads to tempering of the quenched state. A characteristic image of the structure of Hardox 450 steel formed under these conditions is shown in Fig. 1. It is clearly seen that the tempering of steel causes the release of particles of a carbide phase (cementite) located in the volume of the plates and at their boundaries. The particles have an acicular shape, characteristic of cementite formed during the low-temperature tempering of hardened steel [10, 11]. The defect substructure of the martensite plates is represented by dislocations (Fig. 1). Dislocations are either located chaotically (Fig. 2a) or form a mesh substructure (Fig. 2b). The scalar density of dislocations varies within very wide limits, from 3×10^9 to 6.5×10^{10} cm^{-2}. We note that in the martensite crystals of hardened steel, the scalar dislocation density is 10^{11} cm^{-2} [11, 12]. When the steel is heated, the boundaries of the martensite crystals are destroyed, which is especially characteristic of packet martensite (Fig. 2c).

Structure of the contact layer. We call the metal layer located at the interface between the deposited layer and the bulk of the material the contact layer. A polycrystalline structure is revealed on the metal side (Hardox 450 steel), in the volume of grains of which a plate-type substructure is observed (Fig. 3a). Plates are grouped into packets; the transverse dimensions of the plates vary between 150 and 200 nm. High values of the scalar density of dislocations (~4.8×10^{10} cm^{-2}) and the grouping of plates into packets suggest the martensitic (shear) mechanism of their formation.

In the bulk and at the boundaries of the plates, particles of the second phase are revealed (Fig. 3b). Microdiffraction analysis reveals reflections mainly belonging to iron carbide (cementite). The particles have a globular shape; their sizes vary from 20 to 30 nm. We note that in hardened steel, cementite particles have a plate (needle) shape [10, 11]. Consequently, in the contact zone of the deposited layer and the substrate metal, the structure of tempered martensite is formed on the substrate side.

Along with the structure of tempered martensite, grains are present in the contact zone, at joints of boundaries and along the boundaries of which extended layers of the second phase are revealed (Fig. 4).

Dark-field analysis with subsequent assignment of indices of a microelectronogram made it possible to show that the emerging particles are iron boride of the composition FeB (Figs. 4b and 4c). This result means that during the formation of the weld layer, the volume of the adjacent steel layer is doped with elements of the flux-cored wire. The diffusion of alloying elements (namely, boron) proceeds predominantly along grain boundaries, which leads to the formation of iron-boride particles.

On the side of the deposited layer in the contact zone, a structure of the plate eutectic is formed, the characteristic image of which is presented in Fig. 5. The assignment of indices of the microelectronograms obtained for this structure suggests that in the single deposited layer, a eutectic is formed by α-iron and Fe_2B iron borides. In the double deposited layer, the

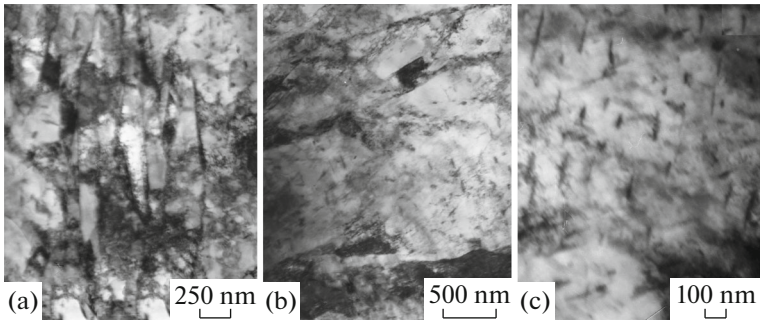

Fig. 1. Electron microscopy image of the structure of Hardox 450 steel, formed in a layer located 15 mm from the surface of the deposited layer.

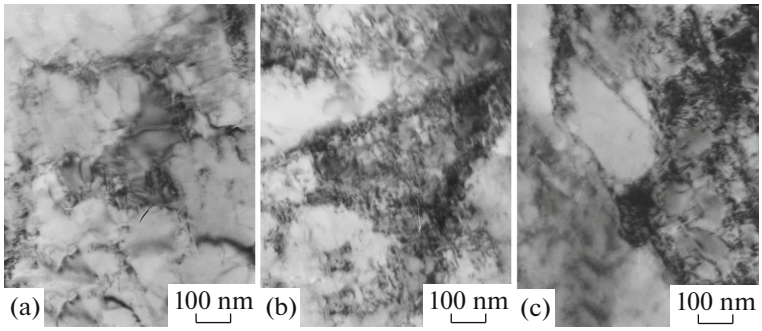

Fig. 2. Defect substructure of Hardox 450 steel, observed in a layer located 15 mm from the surface of the deposited layer.

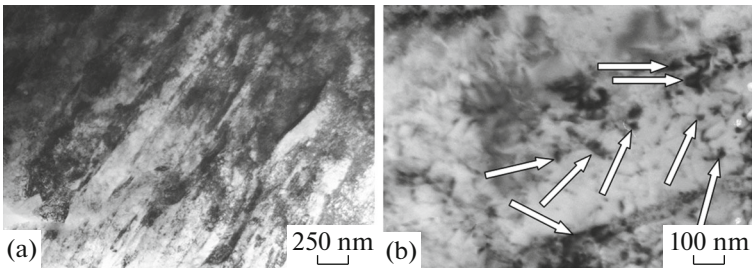

Fig. 3. Structure of the contact layer on the side of Hardox 450 steel; the arrows indicate particles of the second phase.

predominant second phase is iron borides of the composition FeB (Figs. 5a and 5b).

The α phase forming the eutectic of the contact layer in most cases has a structure characteristic of packet martensite (Figs. 5c and 5d). The transverse dimensions of the martensite crystals vary between 50 and 100 nm, which is significantly (3–4 times) smaller than the transverse dimensions of packet martensite crystals detected in the bulk of Hardox 450 steel. The main reason for such significant dispersion of the packet martensite structure of the contact layer is, obviously, a small (0.5–0.8 μm) thickness of iron interlayers at the eutectic point, which undergo a martensitic $\gamma \rightarrow \alpha$ transformation during crystallization and subsequent cooling.

Structure of the deposited layer. The weld layers, both single and double, are characterized by a similar type of structure. The formation of a plate-type eutec-

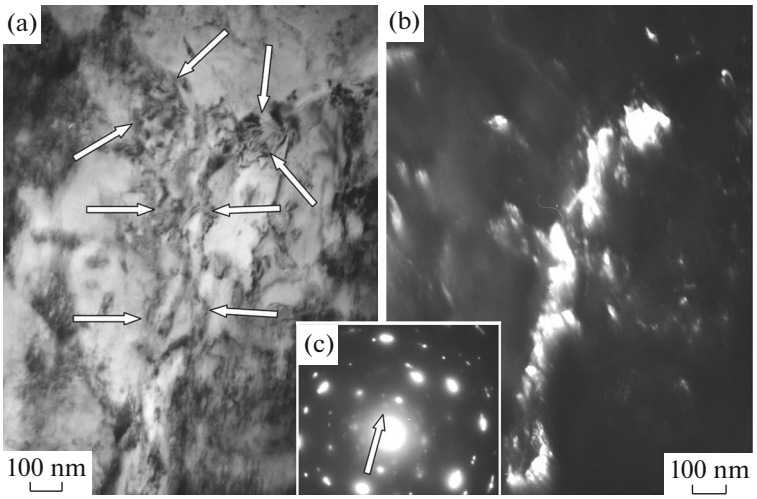

Fig. 4. Electron microscopy image of the structure of Hardox 450 steel in the contact zone with the deposited layer: (a) bright field, (b) dark-field image obtained in the reflection [101]FeB, and (c) microelectronogram (the arrow indicates the reflection, in which the dark field is obtained); the arrows in part (a) indicate the FeB particles located at the junction of three α-phase grains.

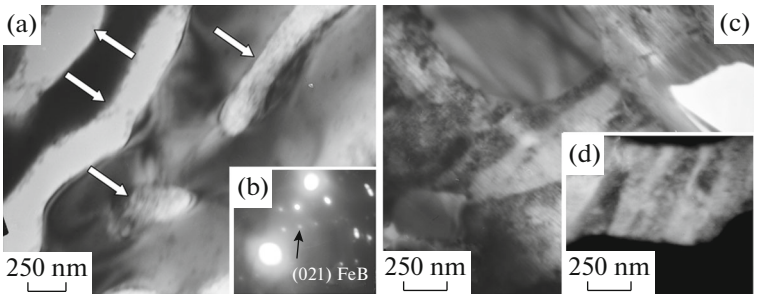

Fig. 5. Structure of the contact layer on the side of the weld metal: (a, c, and d) bright fields and (b) microelectronogram; the arrows indicate the interlayers of the second phase.

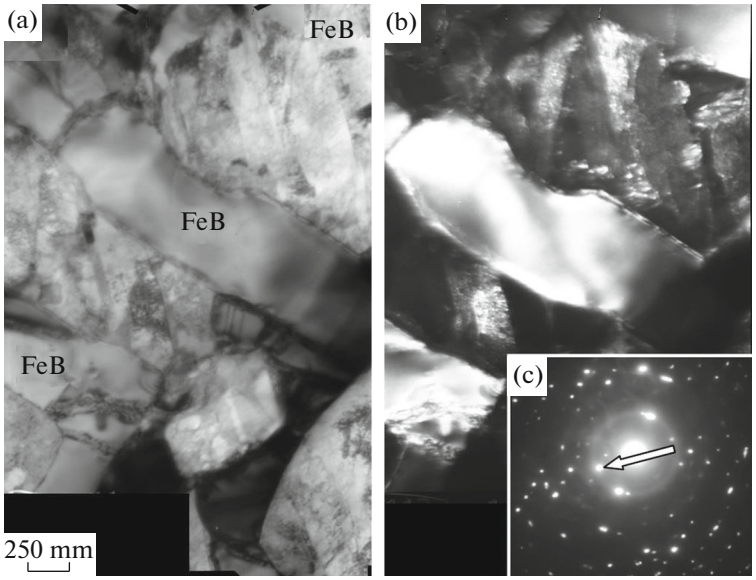

Fig. 6. Electron microscopy image of the structure of a double welded layer: (a) bright field, (b) dark field obtained in reflections [103]FeB + [110]α-Fe, and (c) microelectronogram (the arrow indicates reflections, in which the dark field is obtained).

tic was revealed, the characteristic image of which is shown in Fig. 6.

A feature of the phase composition of the layer deposited in one pass is the formation of plates of iron boride, predominantly, Fe_2B, at the eutectic point. In the double-deposited layer, iron boride of the composition FeB is mainly formed at the eutectic point.

Inclusions of iron boride, regardless of the number of passes during formation of the deposited layer, do not contain a dislocation substructure in their volume, which fundamentally distinguishes them from adjacent layers of the α phase (Fig. 6). The reason for the absence of a dislocation substructure in the plates of iron borides is their relatively high hardness. The hardness of Fe_2B and FeB is 12.5–16.8 and 18.9–23.4 GPa, respectively [13, 14]. A characteristic feature of the electron microscopy image of borides is the presence of inclusions of a large number of bend extinction contours in the volume (Fig. 7, contours are indicated by arrows). The presence of bend extinction contours indicates the formation of internal stress fields in the material, leading to bending–torsion of the crystal lattice [6–9, 11]. The sources of the stress fields (stress concentrators) are interphase boundaries (interfaces of boride and α-phase inclusions) and intraphase boundaries (interfaces of iron borides).

In the formation of the deposited layer in a single pass, the α phase separating plates of iron borides is represented mainly by martensite of packet morphology, the characteristic image of which is shown in Fig. 8a. The transverse dimensions of the plates vary from 30 to 70 nm. A dislocation substructure of the mesh type is observed in the volume of the plates. Judging from the dimensions of the cells of the dislocation grids, the scalar dislocation density is 10^{11} cm^{-2}. The high density of dislocations and the plate morphology of the interlayers indicate a martensitic mechanism of formation of the α phase with the formation of an ultra-fine martensitic structure. For compari-

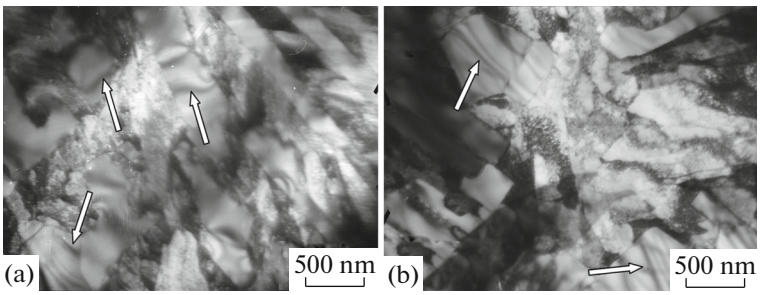

Fig. 7. Structure of the layer deposited (a) in one pass and (b) in two passes; the arrows indicate bend extinction contours.

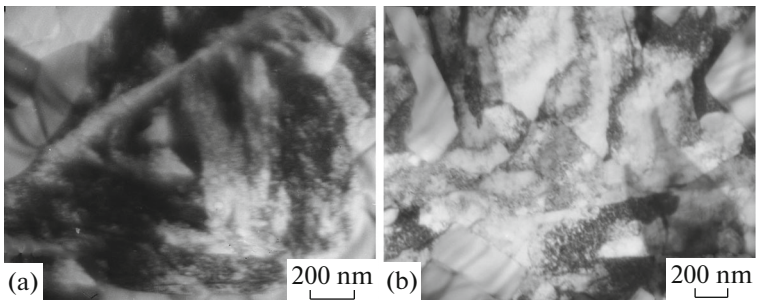

Fig. 8. Structure of the α-phase formed in the layer deposited in (a) one pass and (b) two passes.

son, we note that in hardened steel, the average transverse dimensions of the plates of packet martensite vary within the range of 150–200 nm; the transverse dimensions of plate martensite crystals reach units of micrometers [10–12].

In the layer deposited in two passes, the α-phase structure is more diverse. Along with regions with nanoscale martensite, similar in morphology to martensite formed in a single-weld layer, regions with a subgrain structure are revealed (Fig. 8b). This fact may indicate a change in the rate of cooling of the material during the formation of a reweld layer.

Thus, the performed studies of the structure and phase composition of the deposited layer revealed the formation of a multiphase state characterized by the presence of a large number of inclusions of iron borides, the hardness of which significantly (by more than an order of magnitude) exceeds the hardness of Hardox 450 steel. Obviously, the hardness of the eutectic composition differs from the hardness of iron borides. Indeed, mechanical tests of the material confirmed this assumption.

The results of investigation of the microhardness of the material obtained with single and double deposition of a weld layer (cross section, microhardness profile) are shown in Fig. 9. One can note the formation of a high-strength surface layer, the microhardness of which varies from 10.5 to 12.5 GPa for one pass and is ~15 GPa for a double pass. Therefore, the hardness of the weld layer formed upon one pass is more than twice the hardness of the base metal (Hardox 450 steel) with a thickness of the weld layer of at least 7 mm. Upon a double pass, the hardness of the deposited layer is approximately three times the hardness of the substrate with a thickness of the modified layer of at least 10 mm. The difference in the hardness of the deposited layers is due, as shown by the studies, to the difference in the phase composition of the single and double layers. For one pass in the deposited layer, iron boride of composition Fe_2B is mainly formed, and for a dou-

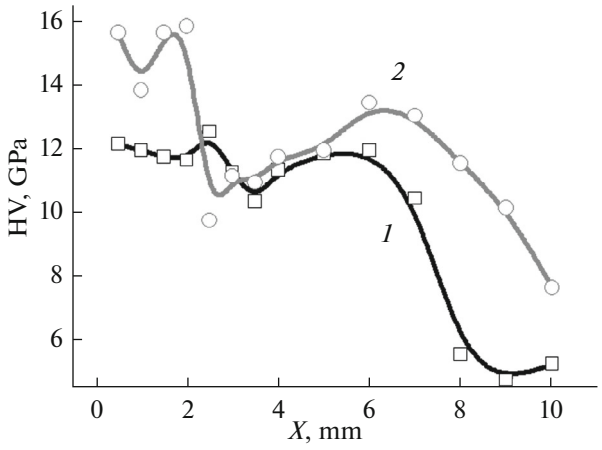

Fig. 9. Microhardness profile of the weld layer–steel system for (*1*) a single deposited layer and (*2*) a double deposited layer.

ble pass, iron boride FeB appears; the hardness of these borides differs by ~1.5 times.

CONCLUSIONS

The phase composition, defect substructure, and mechanical properties of a layer weld on a Hardox 450 steel substrate, formed in a single and double pass, are studied. It is shown that the hardness of the deposited layer depends on the number of passes, and the hardness of the layer obtained in two passes exceeds the hardness of the base metal (Hardox 450) by three times at a thickness of the hardened material of more than 10 mm. It is found that the increased mechanical properties of the deposited layer are associated with the formation of a multiphase submicrostructure and nanoscale structure, the hardening of which is due to the quenching effect (the formation of an ultra-fine martensitic structure of the α phase) and the presence of inclusions of submicrosized borides forming a plate-type eutectic system. It is shown that Fe_2B iron boride is predominantly formed in the single-weld layer; in the double weld layer, FeB iron boride is mainly observed.

ACKNOWLEDGMENTS

The study was supported by the Russian Science Foundation, project no. 15-19-00065.

REFERENCES

1. E. V. Kapralov, E. A. Budovskikh, V. E. Gromov, et al., *Structure and Properties of Composite Wear-Resistance Facings on Steel* (Siberian State Industrial Univ., Novokuznetsk, 2014) [in Russian].
2. E. V. Kapralov, S. V. Raikov, E. A. Budovskikh, et al., Bull. Russ. Acad. Sci.: Phys. **78** (10), 1015 (2014).
3. E. V. Kapralov, S. V. Raikov, E. A. Budovskikh, et al., Fundam. Probl. Sovrem. Materialoved. **11** (3), 334 (2014).
4. Yu. F. Ivanov, V. E. Gromov, E. V. Kapralov, and S. V. Raikov, Fundam. Probl. Sovrem. Materialoved. **11** (4), 515 (2014).
5. V. E. Gromov, E. V. Kapralov, S. V. Raikov, et al., Usp. Fiz. Met. **15**, 211 (2014).
6. D. Brandon and W. D. Kaplan, *Microstructural Characterization of Materials* (John Wiley and Sons, Chichester, 2008).
7. L. M. Utevskii, *Diffraction Electron Microscopy in Metals Science* (Metallurgiya, Moscow, 1973) [in Russian].
8. G. Thomas and M. J. Goringe, *Transmission Electron Microscopy of Materials* (John Wiley and Sons, New York, 1979).
9. P. Hirsch, A. Howie, R. Nicholson, et al., *Electron Microscopy of Thin Crystals* (Butterworth, London, 1965).
10. V. G. Kurdyumov, L. M. Utevskii, and R. I. Entin, *Transformations in Ferrum and Steel* (Nauka, Moscow, 1977) [in Russian].
11. Yu. F. Ivanov, E. V. Kornet, E. V. Kozlov, and V. E. Gromov, *Hardened Structural Steel: Structure and Hardening Mechanisms* (Siberian State Industrial Univ., Novokuznetsk, 2010) [in Russian].
12. Yu. N. Petrov, *Defects and Diffusionless Transformation in Steel* (Naukova Dumka, Kiev, 1978) [in Russian].
13. G. V. Samsonov, T. I. Serebryakova, and V. A. Neronov, *Borides* (Atomizdat, Moscow, 1975) [in Russian].
14. Yu. B. Kuz'ma and N. F. Chaban, *Binary and Triplex Boron-Containing Systems. Handbook* (Metallurgiya, Moscow, 1990) [in Russian].

Translated by O. Zhukova